GRB observations with MAXI

Motoko Suzuki,[1] and MAXI team

[1] Japan Aerospace Exploration Agency, 1-1, Sengen 2chome, Tsukuba, Ibaraki 305-8505, Japan
E-mail(MS): suzuki.motoko@jaxa.jp

ABSTRACT

MAXI has an ability to distribute gamma-ray burst (GRB) alert promptly. For the prompt emissions, bursts in the MAXI field of view (1.5deg × 160deg × 2ways) will be observed. Based on latest results of observations, we simulate various prompt emissions and X-ray afterglows of GRBs. From the results of simulations we estimate sensitivity to these bursts. The positions of the bursts (excluding bursts with the angular distance to the sun of <30 deg) will be scanned by MAXI within about 70 minutes of the prompt emissions. GRB prompt emissions or other transient events will be searched by MAXI Nova Search system, and these information will be distributed to the world. In this document, the summary of the number of observable bursts and X-ray afterglows are presented,

KEY WORDS: X-rays: observations — gamma-rays: bursts — methods: simulations

1. Introduction

In studying gamma-ray bursts (GRBs), It is important not only analyzing prompt emissions but also investigating into afterglows and host galaxies with telescopes. Automatic system of the localization from prompt emissions and alert systems to distribute burst information enable the fast and complete follow-up observation. MAXI is a mission which has an ability of fast localization and distribution of alert.

MAXI covers 0.5-30keV energy range. This will provide unique capability to catch extremely soft bursts, called X-ray flashes (XRFs). The study of XRFs are advanced based on the data from BeppoSAX and HETE-2. After the end of HETE-2 operation, MAXI may be the first mission that is able to trigger GRBs or XRFs in energy range below 25 keV. Moreover, joint fit the data of the instruments sensitive to higher energy range, such as BAT on Swift, GBM and LAT on Fermi, and WAM on Suzaku, with MAXI will give more accurate low-energy index for soft bursts, and also accurate E_{peak}.

MAXI consists of two kinds of detectors, position sensitive gas-proportional counters for 2-30 keV X-rays (Mihara et al. 2008) and CCD cameras for 0.5-12 keV X-rays (Tomida et al. 2008). Among the two type of instruments of MAXI, the camera of gas-proportional counters (Gas Slit Camera: GSC) has relatively large effective area and field of view. Considering these properties, we can conclude GSC is more suitable for the detection of GRBs both prompt emissions and X-ray afterglow.

To study how much GRBs are in the MAXI field of view, and the quality of the data from MAXI, we use maxi simulator (Eguchi et al. 2008). First we describe the function of maxi simulator in section 2.1.. Details of models of prompt emissions and X-ray afterglows we simulated will be presented in section 2.2. and section 2.3. respectively. In section 3., the descriptions of method of processing and analyzing data from MAXI simulator are given. In section 4., we discuss the potentiality of MAXI for observations of GRBs, and in section 5. summarize conclusions.

2. Methods and parameters of simulation

2.1. Overview of MAXI simulator

MAXI simulator is a program which simulate MAXI instruments. We can input the list of X-ray sources, including variable sources. The spectra of the sources should be described in the parameter files. When we run the program, simulator considers orbits and attitude of ISS, and then select the sources in the field of view of the instruments. After the decision of the properties of photons coming into the detector, simulator calculates output pulse height using detector response function. Finally, it outputs the list of X-ray events. The format of the output is similar to the raw data from MAXI.

2.2. Simulations of prompt emissions

MAXI simulator accept fast rise exponential decay type "burst model" as a model of variable source light curve. The source flux F of the burst source is given by the following function,

$$F(t) = \begin{cases} 0 & (t < t_0) \\ \exp\left(-(t-t_0)/\tau\right) & (t \geq t_0) \end{cases} , \qquad (1)$$

where t_0 is the time of the peak and τ is the decay time of the burst. We take $\tau = 10$ seconds for burst sim-

ulation. MAXI will observe efficiently rather soft and bright GRBs. Therefore we decided to adopt the spectral parameters of GRB030329 (see Table 1), which is the most bright GRB in the field of view of HETE-2. In order to study the sensitivity of MAXI GSC to GRBs, we changed two parameters, the intrinsic flux and the incident angle of the bursts, both of which affect the intensity of the signal of the burst. The intrinsic peak flux of the burst was changed from 1/300 to 1 of the average flux of GRB030329. To express an incident angle on MAXI cameras, it is convenient to adopt the coordinate drawn in figure 1. Because collimator sheets are parallel to the x-z plane, an effective area to a point source determined mainly by azimuthal angle of a source. On the other hand, changes of elevation angle have little effect on effective area. In the simulations of GRBs, we have to take into account only a peaking time t_0 of a burst instead of azimuthal angle. This is because azimuthal angle changes, in contrast to elevation angle, during a scan of a source.

Figure 2 shows variation of effective area about a point source as a function of the time. As shown in the figure, we defined the offset time of a burst as a time from the peaking time of the effective area curve to the peaking time of the burst. If the burst precede the peak of the effective area curve, the offset takes negative value.

We set the offset time between -34 sec and $+26$ sec.

2.3. Simulations of X-ray afterglows

To simulate X-ray afterglows, first we defined "average" X-ray afterglow. According to comprehensive study of X-ray afterglows observed by Swift (for example Nousek et al. 2006, Sakamoto et al. 2008), X-ray afterglows generally follow the shape shown in the top panel of figure 3. In order to estimate the rate of X-ray afterglows observed with GSC, we should examine how long GSC can observe an X-ray afterglow. A rough estimate may be made considering the flux limit of a source with a scan, which is about 20 mCrab (Hiroi et al. 2008). This limit corresponds to 10^{-9} erg cm^{-2} sec^{-1} in the energy band of X-ray telescope on Swift, 0.3–10 keV. an average X-ray afterglow stays this flux level for only about 150
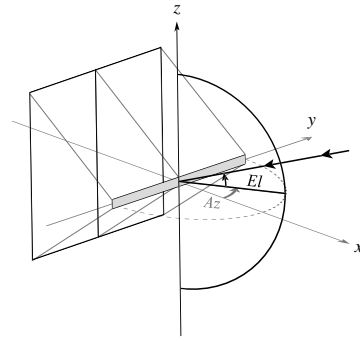

Fig. 1. Definition of the incident angle on GSC. The thin long box in gray is a slit plane of a camera. We define the slit coordinate system of Cartesian coordinate. The slit-normal axis is defined as an axis normal to the slit plane. The slit-long axis is an axis parallel to the long edge of the slit, and slit-short axis is an axis parallel to the short edge of the slit. A path of a photon is defined with two parameters, slit-elevation angle (El) and slit-azimuthal angle (Az). The slit-elevation angle is defined as an angle between the path of a photon and the plane of slit-normal and slit-long axes. The slit-azimuthal angle is an angle between the projection of the path of photon toward the plane of slit-normal and slit-long axes, and slit normal axis. is define as an angle between
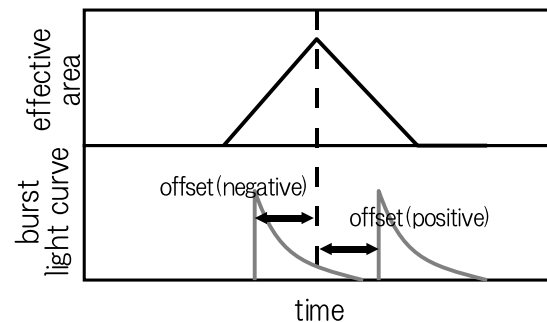

Fig. 2. A schematic picture of the definition of the offset time.

seconds. To confirm this estimation with simulator, we tested four cases: the peak of effective area curve comes 100, 150, 200, and 250 seconds after the burst (the lower panel of figure 3.) The spectral model of the afterglows in the simulations is set to the power-law function with the index -2.0.

2.4. Simulations of X-ray and non X-ray background

One of the most important elements of the simulation is an estimation of background in the MAXI instruments. The estimation and simulation of backgrounds in the instruments are important, because we will discuss the detection and significance of the burst signal against the background. We generate photons of cosmic X-ray background assuming isotropic distribution in the sky. The spectrum and intensity of the background is set to the parameters in Boldt (1987). On the other hand, the
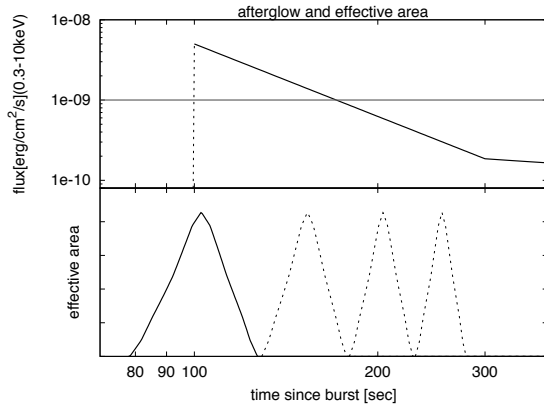
Table 1. The spectral parameters of GRB030329 (Sakamoto et al. 2005). The spectral model is Band function (Band et al. 1993). The normalization is in the unit of 10^{-2} photons cm^{-2} s^{-1} keV^{-1} at 15keV.

model parameter	value
low-energy index α	-1.26
high-energy index β	-2.28
peak energy in νF_ν spectrum E_{peak} (keV)	67.8
normalization	146

Fig. 3. An "average" light curve of X-ray afterglow, and effective area curve, which we tested.
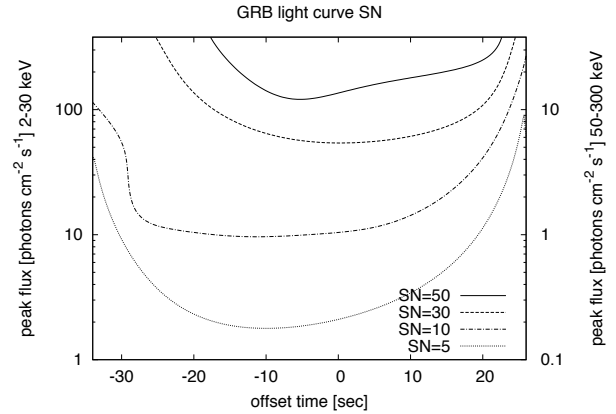

Fig. 4. The contour map of light curve S/N in the space of time offset of the burst and the flux of the burst. The horizontal axis is the offset time, which defined as shown in figure 2. The vertical axis is the flux of the burst. The contour of solid, dashed, dashed-dotted, and dotted line correspond to the S/N level of 50, 30, 10, and 5 respectively.

rate and spectrum of non X-ray background are estimated from the data of ground calibration or the data from other satellites. The count rate of non X-ray backgrounds are set to 10 counts per GSC counter per second. The energy and position distribution of non X-ray background are determined from the background templates, which is based on the data of ground calibration. Note that the rate of non X-ray background will vary with latitude, longitude, and altitude on earth. However, we do not take into account this effect in current simulation.

3.   Process and analysis of simulated data

3.1.   Processing procedure

The data from MAXI simulator is a series of ASCII format files. We process these files to create event files of standard fits format. Then we extract images, light curves, and spectra from event files using *xselect* [1] . To find prompt emission of the bursts, first we generate light curves of certain area of detector coordinate, because a point source stays at the same region in the detector coordinate during a scan. Then we examine these light curves to find excesses from the background rate.

3.2.   Study of the rate

In order to study GRB and afterglow rate, first we have to decide the criterion of "detection" of the bursts. First we introduce the term "light curve S/N", which is defined as the ratio of the counts of the burst photons to the counts of background fluctuation in a time bin. We set the criteria that light curve S/N should be above 5.

3.2.1.   The rate of prompt emissions

The observation rate of bursts is proportional to both observation time window and total rate above the sensitivity. Figure 4 shows the cntour of light curve S/N in

[1] http://heasarc.gsfc.nasa.gov/docs/software/lheasoft/ftools/ xselect/index.html

the space of time offset and burst flux. From figure 4, we can observe the burst with the flux level of 0.4 photons cm^{-2} s^{-1} in 50–300 keV, when the time offset ranges from -25 to $+12$. Next, we have to consider the total rate of GRB. Stern et al. (2002, S02 hereafter) shows the combined BATSE and Ulysses GRB brightness distribution in 50–300 keV range. According to S02, the number of the burst, correspoinding to this flux limit, is about 400 events per year.

Combining the observable time offset range and total rate of the burst, we can calculate the rate of GRBs in the MAXI field of view N_{fov} as the following.

$$N_{\mathrm{fov}} = \eta \left(\frac{t_{\mathrm{win}}}{t_{\mathrm{orbit}}} \right) n_{\mathrm{system}} N_{\mathrm{total}}, \qquad (2)$$

where η is operation efficiency of the MAXI instruments, t_{win} is the observable time offset interval, t_{orbit} is the orbit period of the ISS, and n_{system} is number of camera system, and N_{total} is the total number of GRBs. The operation efficiency η should be about 0.65 due to the scheduled turn off when the sun in the field of view of the camera or at the South Atlantic Anomaly. The orbital period of the ISS t_{orbit} is about 5500 sec. The observable time offset interval t_{win} and the total number of GRBs depend on the flux level of the GRBs. In the case of 0.4 photons cm^{-2} s^{-1} in 50–300 keV, the numbers are

$$\begin{aligned} N_{\mathrm{fov}} &\approx 3.5 \left(\frac{\eta}{0.65} \right) \left(\frac{t_{\mathrm{win}}}{37} \right) \\ &\left(\frac{5500}{t_{\mathrm{orbit}}} \right) \left(\frac{n_{\mathrm{system}}}{2} \right) \left(\frac{N_{\mathrm{total}}}{400} \right). \qquad (3) \end{aligned}$$

3.2.2.   The rate of afterglows

The observable rate of GRB afterglow in the GSC field of view is mainly determined with the length of X-ray af-
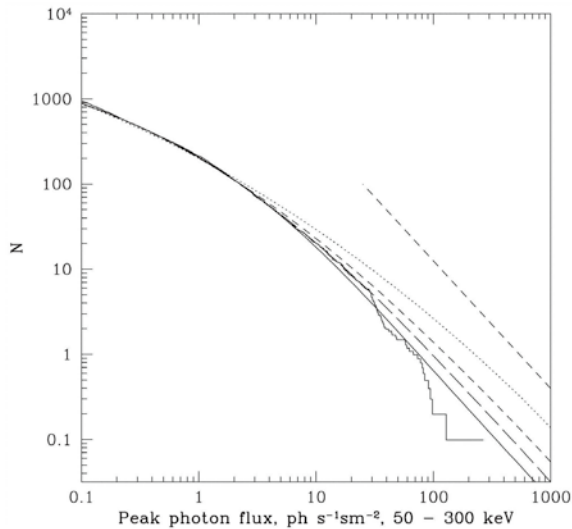
Fig. 5. The integral peak flux distribution of Ulysses/BATSE GRBs. This figure is from Stern et al. (2002).

terglow staying above the detection limit of a scan. From the result of our simulations, the average afterglow is too dim to detect with GSC even after 150 seconds after the prompt emission. It is necessary to scan the position of the afterglow within 100 seconds after the prompt emission. From the similar calculation to equation (3), we can estimate the rate of X-ray afterglows as

$$N_{\text{fov}} \approx 2.4 \left(\frac{\eta}{0.65}\right) \left(\frac{f}{0.1}\right) \left(\frac{t_{\text{win}}}{100}\right)$$
$$\left(\frac{5500}{t_{\text{orbit}}}\right) \left(\frac{n_{\text{system}}}{2}\right) \left(\frac{N_{\text{total}}}{1000}\right), \qquad (4)$$

where f is indefinite fraction of bursts with bright X-ray afterglows.

4.   Discussions
4.1.   GRBs, afterglows, and other transients
It takes less than 50 seconds for a star to cross the MAXI field of view. In other words, the maximum exposure time of a star in a scan is less than 50 seconds. The first alert of MAXI bursts should be sent based on the data of this small exposure time. The following observation of the burst by MAXI itself must be delayed for 20 or 70 minutes. It is difficult to classify the transient event into burst, afterglows, or other class of events only from the information of such short exposure.

4.2.   Uncertainty about the rate of soft bursts
As of now, the largest collection of the bursts is BATSE burst catalog (Paciesas et al. 1999). To calculate the burst rate in the MAXI field of view, we used S02, which contains the samples of Ulysses in addition to the BATSE samples. It should be noted that the rate in the S02 is

the rate in 50 – 300 keV energy range. On the other hand, MAXI GSC covers 2 – 30 keV, which is an order of magnitude softer than BATSE's or Ulysses's band. We extrapolated the relation between the rate and the brightness in 2 – 30 keV band from the rate of S02 using the spectrum of the burst with intermediate hardness. According to Sakamoto et al. 2005, one third of the bursts emit more energy in X-ray (2 – 30 keV) band than gamma-ray (30 – 400 keV) band. Therefore some of the dim burst in 50 – 300 keV band should emit more energy in 2 – 30 keV, which may be easily detected with MAXI GSC.

4.3.   Suggestion on the high redshift GRBs
Generally bursts originate from high redshift should have soft spectra and long duration. These properties are at advantages in observing high redshift GRBs with MAXI. As shown in equation (3), the burst rate in the MAXI field of view is proportional to the observable time window t_{win} within an orbit. This t_{win} heavily depends on the duration of the burst. Of course, the cameras with low energy sensitivity are also suitable to observe soft events. Moreover, the capability of imaging is unique to MAXI. It is difficult to trigger less variable source with a detector of coded mask type, which is common to WFC on BeppoSAX, WXM and SXC on HETE, and BAT on Swift.

5.   Conclusions
MAXI will be able to detect 3.5 prompt emissions and 2.4 X-ray afterglows of GRBs per year. About prompt emissions, the uncertainty of the number mainly comes from the ambiguous extrapolation of the rate from gamma-ray to X-ray band. On the other hand, the uncertainty of the rate of the afterglows comes from uncertainty of the brightness distribution of the X-ray afterglows.

MAXI GSC has intrinsic capability of imaging and sensitivity in relatively low energy band. These properties will be advantages in detecting high redshift GRBs.

References
Band, D. et al. 1993, ApJ, 413, 281
Boldt, E. 1987, Observational Cosmology, 124, 611
Eguchi, S. et al. 2009, in this proceedings
Hiroi, K. et al. 2009, in this proceedings
Mihara, T et al. 2009, in this proceedings
Nousek, J. A. et al. 2006, ApJ, 642, 389
Paciesas, W. S. et al. 1999, ApJS, 122, 465
Sakamoto, T. et al. 2005, ApJ, 629, 311
Sakamoto, T. et al. 2008, ApJ, 679, 570
Stern, B. E. et al. 2002, ApJ, 578, 304
Tomida, H. et al. 2009, in this proceedings